Evolution of Stellar Objects According to J. Wheeler's Geometrodynamic Concept

Anatoly V. Belyakov
E-mail: belyakov.lih@gmail.com

The proposed model is based on J. Wheeler's geometrodynamic concept, in which space continuum is considered as a topologically non-unitary coherent surface admitting the existence of transitions of the input-output kind between distant regions of the space in an additional dimension. The existence of closed structures (macrocontours) formed at the expense of interbalance of gravitational, electric, magnetic and inertial forces has been substantiated. It is such macrocontours that have been demonstrated to form — independently of their material basis — the essential structure of stellar objects (SO) and to determine the position of these objects on the Hertzsprung-Russell diagram. Models of the characteristic types of stellar objects: stars and compact bodies emerging in the end of stellar evolution — have been presented, and their standard parameters at different stages of evolution have been calculated. The existence of the Hertzsprung-Russell diagram has been substantiated, and its computational analogue has been given. Parallels between stellar and microcosmic objects are drawn.

> Recognizing the Seeker, Nature itself will come to meet him.
>
> *Rockwell Kent*

1 Introduction

Wheeler's geometrodynamic concept, in which microparticles are considered as vortical oscillating deformations on a non-unitary coherent surface, was earlier used by the author to construct model objects of the microcosm [1, 2]. Those works substantiated the existence of closed structures (contours), determining the properties of microparticles. At the same time, the idea about transitions between distant regions of space in the form of Wheeler's "wormholes" can be extended to the scale of macrocosm, and some contemporary astrophysical theories has already made use of it [4]. In this paper, the existence of closed contours is substantiated at the cosmological scale, and grounds are given that they make the basis of stellar objects (SO).

The work does not consider the nature of the cosmological medium that forms stellar bodies, nor it does the nature of mass/charge carriers, force interactions etc., or various physical *manifestations* of the evolutionary behavior of stellar objects. These tasks are a subject of specific disciplines.

The model presented in the paper has an outline, illustrative character and suggests a new look at the problem. For the model, the only important thing is the *existence* of the aforementioned *entities*, forming certain types of stellar structures and determining their evolution. The work does use specific SO terms, but only schematic SO models are considered, with their evolution depending only on a few parameters reflecting the most important features of the real objects.

The SO models used here are based on the balance between main interactions: electrical, magnetic, gravitational and inertial — with no additional coefficients introduced. The analysis gives good qualitative results and, in a number of cases, plausible quantitative parameters for the statistically averaged (typical) stellar objects.

2 Initial premises

As was shown earlier [1], from the purely mechanistic point of view the so-called *charge* only manifests the degree of the nonequilibrium state of physical vacuum; it is proportional to the momentum of physical vacuum in its motion along the contour of the vortical current tube. Respectively, the *spin* is proportional to the angular momentum of the physical vacuum with respect to the longitudinal axis of the contour, while the *magnetic interaction* of the conductors is analogous to the forces acting among the current tubes.

It is given that the elementary unit of such tubes is a unit with the radius and mass close to those of a classical electron (r_e and m_e).

It should be noted that in [1, 2] the expressions for the electrical and magnetic forces are written in a "Coulombless" form, with charge replaced by electron limiting momentum. In this case, the electrical and magnetic constants (ε_0 and μ_0) are expressed as follows:

$$\varepsilon_0 = \frac{m_e}{r_e} = 3.33 \times 10^{-16} \text{ kg/m}, \tag{1}$$

$$\mu_0 = \frac{1}{\varepsilon_0 c^2} = 0.0344 \text{ N}^{-1}. \tag{2}$$

The electrical constant here is, in fact, the linear density of the vortex tube, with the mass:

$$m = \varepsilon_0 \, l \,, \tag{3}$$

where l is the length of the vortex tube (thread) or contour.

To combine the interactions, let us express them in a dimensionless form with the common force dimension factor $\frac{1}{\mu_0}$. Taking into account (1) and (2),

$$F_e = \frac{1}{\mu_0}\left(\frac{r_e}{r_0}\right)^2 z_{e_1} z_{e_2}, \tag{4}$$

$$F_m = \frac{1}{\mu_0}\frac{l}{2\pi r_0}\frac{r_e^2}{(c\times[\mathrm{sec}])^2} z_{e_1} z_{e_2}, \tag{5}$$

$$F_g = \frac{1}{\mu_0}\frac{1}{f}\left(\frac{r_e}{r_0}\right)^2 z_{g_1} z_{g_2}, \tag{6}$$

$$F_i = \frac{1}{\mu_0}\frac{r_e}{r_0}\left(\frac{\mathrm{v}_0}{c}\right)^2 z_g, \tag{7}$$

where v_0, r_0, z_e, z_g, f are the rotary velocity and rotary radius or distance between the vortex tubes, the relative values of charge and mass in the parameters of electron charge and mass and the ratio of electrical-to-gravitational forces, which, under the given conditions, is expressed as follows:

$$f = \frac{c^2}{\varepsilon_0 \gamma} = 4.16\times 10^{42}, \tag{8}$$

where γ is the gravitational constant.

The *balance of electrical and magnetic forces* $F_e = F_m$ gives a geometrical mean, a characteristic linear parameter that is independent of the direction of the vortex tubes and the number of charges

$$R_\odot = \sqrt{r_0\, l} = \sqrt{2\pi}\, c\times[\mathrm{sec}] = 7.52\times 10^8 \text{ m}, \tag{9}$$

a magnitude close to the Sun radius and the sizes of typical stars.

The *balance of magnetic and gravitational forces* $F_m = F_g$ also results in a geometrical mean:

$$\sqrt{r_0\, l} = \sqrt{\frac{z_{g_1} z_{g_2}}{z_{e_1} z_{e_2}}}\sqrt{\frac{2\pi}{f}}\, c\times[\mathrm{sec}] = \sqrt{\frac{\varepsilon}{f}}\, R_\odot, \tag{10}$$

where the ratio of the products $\varepsilon = z_{g_1} z_{g_2}/z_{e_1} z_{e_2}$ is an *evolutionary parameter*, which characterizes the state of the medium and its changes, as the mass carriers become predominant over the electrical ones and, as a matter of fact, shows how the material medium differs from vacuum.

In the general case, expression (10) gives a family of lengthy contours, consisting of contra-directional closed vortex tubes (*m_g-contours*). The evolutionary parameter ε proportionally increases the mass of the vortex tube for the m_g-element:

$$m = \varepsilon\varepsilon_0\, l. \tag{11}$$

The vortex tubes can consist, in their turn, of a number of parallel vortex threads, whose stability is ensured by the *balance of magnetic and inertial forces* ($F_m = F_i$; *m_i-zones*). As follows from this balance,

$$\mathrm{v}_{0i} = \sqrt{\frac{z_{e_1} z_{e_2}}{z_g}}\sqrt{\frac{r_e\, l}{2\pi}}\times[\mathrm{sec}^{-1}]. \tag{12}$$

Unidirectional vortex threads of the length l rotate, with the rotary velocity v_{0i}, about the longitudinal axis along an orbit of indeterminate radius. When they are filled with the chains of single charges, having the mass of an electron, and their number $z_e = z_g = l/r_e$ (or when the tubes consist of single vortex threads in the quantity of l/r_e), we get the following equation:

$$\mathrm{v}_{0i} = \frac{l}{\sqrt{2\pi}}\times[\mathrm{sec}^{-1}]. \tag{13}$$

The *balance of gravitational and inertial (centrifugal) forces* $F_g = F_i$ gives a *virial*, from which one can derive the maximal gravitational mass of the object, satisfying condition (9):

$$M_m = \frac{R_\odot c^2}{\gamma} = f R_\odot \varepsilon_0 = 1.012\times 10^{36} \text{ kg}. \tag{14}$$

3 Structurizations of the primary medium and parameters of stellar objects

Now let us consider objects in which more than one pair of forces is balanced.

Let us assume that an initially unstructured maximal mass evolves and becomes more complex — through the emergence of m_i-zones, consisting of single elements of the length l_i and mass m_i. As follows from the constancy of μ_0 in the general case,

$$\frac{1}{\mu_0} = \varepsilon_0 c^2 = \frac{m_i \mathrm{v}_{i_0}^2}{r_i} \tag{15}$$

where $m_i = \varepsilon_0 l_i$ is the mass of a vortex m_i-element. From (13) and (15), one can obtain, having in mind (9), the ratio for its geometrical parameters:

$$\frac{l_i^3}{r_i} = R_\odot^2. \tag{16}$$

Driven by gravitation, the single tubes (threads) will combine into a local structure, the mass of which can also be calculated from the virial:

$$M_i = \frac{r_i \mathrm{v}_{i_0}^2}{\gamma}. \tag{17}$$

Let the object contain z_i local zones; then its mass will be $M_0 = z_i M_i$. Let us introduce a dimensionless parameter

$M = M_0/M_m$. Then, making some transformations, one can eventually obtain uniform equations for all the parameters of the evolving objects with an arbitrary relative mass M:

number of local zones

$$z_i = \frac{1}{M^{1/4}}\,, \tag{18}$$

zone radius

$$r_i = M^{3/4} R_\odot\,, \tag{19}$$

length of the vortex tube (thread)

$$l_i = M^{1/4} R_\odot\,, \tag{20}$$

rotary velocity in the zone

$$\mathrm{v}_{0i} = M^{1/4}\, c, \tag{21}$$

number of single vortex threads in the zone

$$n = \frac{M_i}{m_i} = f M\,, \tag{22}$$

and, having in mind (10), one can take $n = \varepsilon$.

Thus, as its mass decreases, the *object simultaneously becomes more and more complex*, getting subtly structured with m_i-zones.

Let us assume that the initial state of SO is a rotating disk, which can further develop into larger structures (m_g-contours) of the size $R_0 \times d_0$, where the contour length is $R_0 = l$ and diameter is $d_0 = r_0$. With these designations, equation (10) will look as follows:

$$\sqrt{d_0\, R_0} = \sqrt{\frac{\varepsilon}{f}}\, R_\odot\,. \tag{23}$$

Let us accept, quite schematically and roughly, that m_g-contours in the disk are oriented radially-spirally and are pulled in towards the center by the radial components of the gravitational forces. These forces are approximately equal to $(d_0/R_0)F_g$. Then, from the balance of centrifugal and gravitational forces,

$$\mathrm{v}_0 = \sqrt{\frac{d_0}{R_0}}\,\sqrt{\frac{\gamma m}{R_0}}\,, \tag{24}$$

where m and R_0 are the m_g-contour mass and the averaged disk radius respectively.

Let us define the number of m_g-contours as

$$z_0 = \frac{R_0}{d_0}\,. \tag{25}$$

With equation (11) in mind, the total mass of the object will amount to

$$M M_m = z_0\, m = z_0\, \varepsilon \varepsilon_0\, R_0. \tag{26}$$

Taking into account equations (8), (9), (23–26) and making some transformations, we can find parameters of the structured disk:

$$R_0 = M^{1/3}\, R_\odot\,, \tag{27}$$

$$z_0 = \frac{f M^{2/3}}{\varepsilon}\,, \tag{28}$$

$$\mathrm{v}_0 = \frac{\varepsilon c}{f M^{1/3}}\,. \tag{29}$$

The parameters found are averaged when the disk structural elements are tightly packed, and they determine the core of the object. Let us define the object boundaries — under the condition that, if the system of m_g-contours is rotating as a rigid disk, the rotary velocity of contours at the periphery must not exceed the speed of light. In this case, the maximal radius of the disk will be:

$$R_m = \frac{R_0\, c}{\mathrm{v}_0} = z_0\, R_\odot\,. \tag{30}$$

Let us further assume — within the framework of our simplified model — that the mass of the object is concentrated either in the center (the *state of core*) or at the periphery (the *state of outer layer*). Obeying the angular momentum conservation law, velocity at the periphery cannot be higher than:

$$\mathrm{v}_m = \frac{\mathrm{v}_0 R_0}{R_m} = \frac{\mathrm{v}_0^2}{c}\,. \tag{31}$$

Let the periods of core and outer layer rotation be expressed as $\tau_0 = R_0/\mathrm{v}_0$ and $\tau_m = R_m/\mathrm{v}_m$ respectively (the duration of the inner and outer cycles).

Having in mind (27–31) and taking into account that $\sqrt{2\pi} = 2.51$, we obtain

$$\tau_0 = 2.51 M^{2/3} \frac{f}{\varepsilon}, \tag{32}$$

$$\tau_m = 2.51 M^{4/3} \left(\frac{f}{\varepsilon}\right)^3\,. \tag{33}$$

Indeed, star cores rotate much faster that their outer layers [5]. As the medium condenses and becomes more and more different from vacuum, the evolutionary parameter ε grows. There are at least two characteristic values of this parameter satisfying the following conditions:

1. The number of m_g-elements z_0 is equal to the number of m_i-structures z_i, which should correspond to the most stable or *balanced* state of SO in the process of its evolution. In this case ($z_i = z_0$) — as it follows from (18) and (28),
$$\varepsilon = f\, M^{11/12}\,. \tag{34}$$
2. The number of m_g-elements is reduced to one, which will include all the m_i-structures. This state corresponds to the end of a certain period of object's evolution, i.e., to the *degenerate* state. Here, from (28),
$$\varepsilon = f M^{2/3}\,. \tag{35}$$

In the state of degeneration, when $z_0 = 1$, the period of core rotation will — as follows from (30), (32), (35) — be constant for any masses and amount to 2.51 sec, whereas the size of the outer layer will be equal to the standard radius $R_\odot$. In the general case, one can write, combining (34) and (35):

$$\varepsilon = fM^k\,, \tag{36}$$

where the parameter $k \geqslant 2/3$.

Visible dimensions of stars, i.e., radii of their photospheres, depend on many a specific factor; as a rule, they do not equal to the radius R_m and can be evaluated only roughly. The same can be said about star temperatures. Let us take the mass of the Sun as a standard (the validity of such a choice will be justified later) and consider the radius of the solar photosphere being close to $R_\odot$. Then, within the limits of the main sequence for the stable state and taking into account our disk model, the relative radius of the photosphere R_f for a star of arbitrary mass can be expressed via the mass of the Sun. It is evident that for a *two-dimensional* model,

$$R_f = \left(\frac{M}{M_\odot}\right)^{1/2} \tag{37}$$

and in the general case,

$$R_f = \left(\frac{M}{M_\odot}\right)^{i}\,, \tag{38}$$

where $i = 1\ldots1/3$ is a coefficient reflecting the density of packing of m_g-contours in the object.

To evaluate the model object temperature, let us consider its radiation as that of black body. Let the maximal temperature of radiation be achieved at the Compton wavelength of electron, $k = 2.426 \times 10^{-12}$ m, and let us assume that the radiation wavelength is inversely proportional to the rotary velocity of the contour vortex tubes at a given radius. Then, from Wien's formula,

$$T = \frac{b}{\lambda}\,, \tag{39}$$

where $b = 0.0029 \times 10^6$ m $\times\,^\circ$K. Having in mind this proportion, the radiation temperatures at the radii of core and photosphere (and an arbitrary radius as well) can be expressed as

$$T_0 = T_k\left(\frac{\mathrm{v}_0}{c}\right) \tag{40}$$

and

$$T_f = T_k\left(\frac{\mathrm{v}_0}{c}\right)\left(\frac{R_0}{R_f}\right), \tag{41}$$

whereas the energy of radiation (here and so forth, in keV) as

$$E = 511\frac{\mathrm{v}_0}{c}\ \text{keV}, \tag{42}$$

where T_k is the limiting temperature, corresponding to λ_k and equal to $1.19 \times 10^9\,^\circ$K.

Parameters	Balanced state	Degenerate state
ε	2.47×10^{37}	6.56×10^{38}
z	26.6	1
The core		
R_0	0.0126	0.0126
v_0	4.7×10^{-4}	0.0126
τ_0, sec	66.9	2.51
$T_0\,^\circ$K	5.6×10^5	1.5×10^7
The outer layer		
R_m	26.6	1
v_m	2.21×10^{-7}	1.57×10^{-4}
τ_m, sec	$3 \times 10^8 = 9.6$ years	$1.58 \times 10^4 = 4.4$ hours
$T_m\,^\circ$K	263	1.89×10^5
The photosphere		
R_f	1	1
$T_f\,^\circ$K	7050	1.89×10^5

Table 1: Note — radii and velocities are expressed as fractions of $R_\odot$ and c.

4 Model adequacy

It seems improbable that such a schematic and simple model would yield plausible results towards stellar objects. Yet it does. Let us calculate some parameters of a *solar-mass star*. The mass of the Sun equals to 2×10^{30} kg; in relative units, upon division by M_m, $M_\odot = 2 \times 10^{-6}$.

Table 1 shows the results of calculations according to the formulas given above.

In our notation, *angular momentum* of the Sun is equal to

$$0.4(2 \times 10^{30})\,\mathrm{v}_0\,R_0 = 0.4\,M_\odot^{23/12} M_m c\,R_\odot = \\ = 1.09 \times 10^{42}\ \text{kg m}^2/\text{sec}\,, \tag{43}$$

where the coefficient 0.4 takes account of the spherical shape of the body.

Comparing the calculated equilibrium-state parameters of this averaged standard object (a solar-type star) with the actual parameters of the Sun, one can see a close correspondence between their sizes, surface and core temperatures and periods of the solar cycle activity. The Sun's angular momentum is calculated with almost *perfect precision*.

By the end of evolution, upon reaching the degenerate state (at $z_0 = 1$), the periods of the inner (τ_0) and outer (τ_m) cycles diminish to their limits (Table 1). In this case, the single-thread spiral structure would flatten into a disk — thick as the size of the core (R_0) and radiating to the sector of the disk plane. The period of radiation will be $\tau_m = 4.4$ h; impulse duration, $\tau_0 = 2.5$ sec; and temperatures of the core and outer layer correspond to energies, 6.4 and 0.08 keV respectively.

The presence of m_i-zones in the m_g-contour will bring uncertainty into the period of radiation, which will be inversely proportional to the number of m_i-zones. For an object of the solar mass, the uncertainty in the period of impulses will amount to $\tau_m/z_i = 4.4\,h/26.6 = 598$ sec.

These parameters are typical and correspond well to the *x*-ray sources, *barsters*. For example, they perfectly fit the parameters of the X-ray source 3U 1820-30 in the globular cluster NGC6624 [5] etc.

Of course, the model presented here reflects only some essential features of stellar object structure. A stellar object can consist of toroids (balance of magnetic and gravitational forces), whose current-conducting elements rotate above the closed longitudinal axis of the tor (balance of magnetic and inertial forces), whereas the toroids themselves are oriented in the plane of the rotating disk (balance of gravitational and inertial forces). Such a system should hardly be stable. The core would rotate faster than the periphery, and the m_g-contours would coil up, with their kinetic energy transforming into other forms (and then, probably, transforming back). Describing such a system as a multiturn plane-spiral mechanical pendulum might be nave, yet in any case, there should take place an *oscillatory process of the object's gravimagnitodynamical structure*. Indeed, the paired dark spots in the equatorial zone of the Sun seem to be the outlet of m_g-contours — undergoing magnetic reversal and changing their intensity and polarity with the period of 11 years. Their registered quantity (from several to a hundred) does not contradict the calculated mean $z_0 = 26.6$.

Now let us calculate the *density of the SO core*. In the atoms of stellar matter (hydrogen, for the most part), substance circulates, according to our model, within $p^+ - e^-$ — contours with the mass $\varepsilon_0\, r_0$, and circulation speed cannot be higher than that of light [1].

At the same time, the magnitude of the charge e_0 is constant at any quantum number and equals to the momentum of the contour mass $\varepsilon_0\, r_0\, \mathrm{v}_0$. At $\mathrm{v}_0 \to c$, $r_0 \to r_{0\,min}$, therefore

$$r_{0\,min} = \frac{e_0}{\varepsilon_0\, c} = 1.65 \times 10^{-12}\ \mathrm{m}\,. \qquad (44)$$

The density of maximally condensed hydrogen atoms will amount (for a spherical volume) to

$$\rho_{max} = \frac{3m_H}{4\pi r_{0\,min}^3} = 8.82 \times 10^7\ \mathrm{kg/m^3}\,, \qquad (45)$$

where m_H is the mass of a hydrogen atom.

Now let us represent the mean density of the core matter as a ratio of the core mass to its cubic radius. Having in mind the corresponding expressions, one can see that the density is invariable and depends only on the gravitational constant:

$$\rho_0 = \frac{MM_m}{R_0^3} = \frac{M_m}{R_\odot^3} = \frac{1}{2\pi\gamma \times [\mathrm{sec}]^2} = \\ = 2.38 \times 10^9\ \mathrm{kg/m^3}\,. \qquad (46)$$

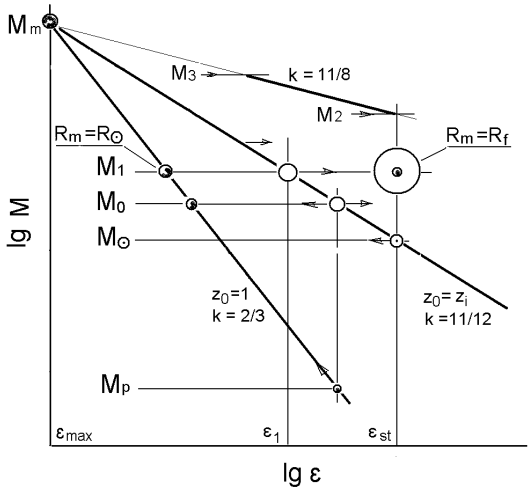

Fig. 1: The diagram "evolutionary parameter — mass".

As follows from the density ratio, a volume equal to that of a single hydrogen atom should contain 27 atoms of the initial matter, which corresponds, by the number of protons, to atoms of the iron group. The density is typical for white dwarfs, such as the famous Kuiper star.

It is interesting that the parameters obtained: $R_\odot$, ρ_0 and $\tau_0 = 2.51$ sec — practically indistinguishable from the values that should characterize the neck of a hypothetical magnetic "wormhole" of the mass M_m [4].

5 Analogues of the Hertzsprung-Russell (H-R) diagram and their applications

The Hertzsprung-Russell (H-R) diagram shows the evolutionary position of stellar objects on the "spectral class (temperature) — luminosity" coordinate plane. Let us consider its analogues: diagrams "evolutionary parameter — mass", and "temperature — mass".

5.1 The diagram "evolutionary parameter — mass"

On such a diagram (Fig. 1), $\varepsilon(M)$ dependencies would better be plotted on a logarithmic scale. At any k, the diagram rays converge on a point corresponding to the limiting mass M_m and limiting evolutionary parameter $\varepsilon_{max} = f$.

Specific parameters of SO will depend on the position of the object on the diagram. In general, with the converging point M_m approached then, as follows from (27–33), (40), (41), the number of m_g-contours will tend to 1; the rotary velocity, to the speed of light; the core and outer layer radii, to $R_\odot$; the periods of the inner and outer cycles, to 2.51 sec; and the core and outer layer temperatures, to T_k.

Evidently, for any given SO, the course of evolution may go both towards larger ε values (condensation of medium), up to $z = 1$, and smaller ε values (depression of medium), up to the shedding of the envelope at the end of the evolutionary process. ***Using the microcosm analogies, one can compare***

these states to the Bohr and ionized atoms respectively.

Let consider a stellar object which is in the main sequence and has a value of the evolutionary parameter corresponding to the line of equilibrium at $k = 11/12$. At $\varepsilon = const$, the equilibrium mass M_0 will correspond to a smaller mass M_p on the line of degeneration, for which $k = 2/3$ and $z_0 = 1$ (Fig. 1). In this case, one can obtain a mass ratio from (34) and (35):

$$M_p = M_0^{11/8} . \tag{47}$$

Since the mass of the Sun is considered standard, we shall take the evolutionary parameter value on the line of equilibrium for the solar mass ε_{st} as standard too.

5.2 Collapsing red giants

At the end of their evolution, stars become red giants and then shed their envelope (transfer to the state of the core), turning to white dwarfs, neutron stars or, in the case of the largest masses, "black holes".

Let us consider a star of chosen characteristic mass, for which every m_g-contour on the line of equilibrium has the mass of the Sun, i.e., satisfying the condition $M_0 = z_0 M_\odot$. Taking into account (28) and (34), we obtain $M_0 = M_\odot^{4/5} = 2.76 \times 10^{-5} = 13.8$ s.m. (masses of the Sun). Let us calculate the typical mass of a white dwarf forming from the core of such a star. Let us assume that on the line of star equilibrium, its core (and, therefore, the mass M_p as well) are on the line of degeneration (Fig. 1). Then, having in mind (47),

$$M_p = M_0^{11/8} = M_\odot^{11/10} = 5.38 \times 10^{-7} , \tag{48}$$

which corresponds to 0.27 s.m.

After the envelope and core are separated, they can be considered discretely. Let the envelope evolve to a standard parameter ε_{st}, and the core delay at the critical stage of the transformation process. Combining these states, let take the white dwarf mass M_p be proportional to the number of m_g-contours z_p — of the total number of m_g-contours z_0 of the mass M_0 at ε_{st}:

$$M_p = \frac{M_0 z_p}{z_0} . \tag{49}$$

Having in mind (28), (34) and (48), one can find the number of m_g-contours in the core:

$$z_p = \frac{f M_0^{25/24}}{\varepsilon_{st}} = M_\odot^{-1/12} = 2.98. \tag{50}$$

Therefore, the total mass of the star will be equivalent to $M_0/M_p = M_0^{-3/8} = M_\odot^{-3/10} = 51.2$ white dwarf masses, which corresponds to the number of nucleons in the nucleus of iron (more precisely, if $z_p = 3$, then $M_\odot = 1.9 \times 10^{-6}$ and the number of "nucleons" is equal to 52). Here we see another analogy with the microcosm: ***a standard red giant, containing 52 white dwarf masses, and a white dwarf, containing three***

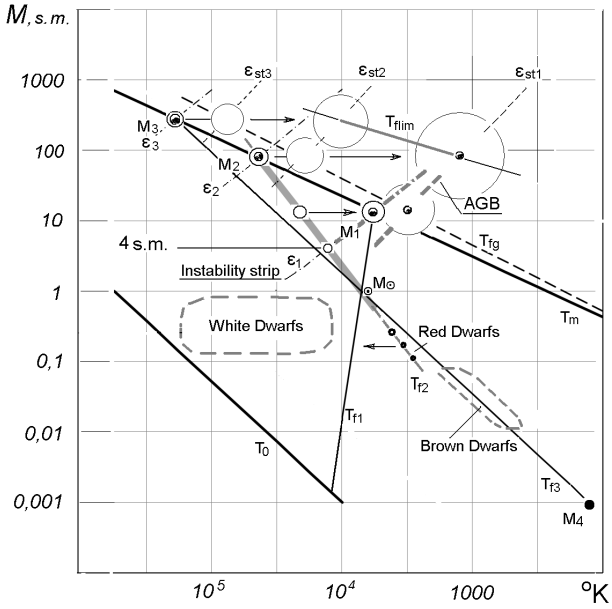

Fig. 2: The diagram "temperature-mass".

m_g-contours, will match an atom of iron, containing 52 nucleons, and a nucleon, consisting of three quarks. Later, other analogies with the microcosm will come into view.

Thus, it seems that the mass of the Sun and its evolutional parameter ε_{st} on the line of equilibrium are, indeed, standard. At $z_0 = 3$, the parameter $k \approx 0.75$, and it changes slightly in a wide range of masses. One can, therefore, expect that the condition (50) is optimal for other masses as well. Then, from (50),

$$\varepsilon_{st} = \frac{f M_0^{25/24}}{3} . \tag{51}$$

5.3 The diagram "temperature-mass"

Since logarithms of luminosity and mass are approximately proportional within the limits of the main sequence, it would be convenient to draw the H-R diagram analog in the coordinates of "temperature — mass".

From (27–30), (34), (40) and (41), one can obtain expressions of the $T(M)$ form, corresponding to the equilibrium temperatures at the radii of the outer layer R_m and core R_0 at $k = 11/12$. On a logarithmic scale (Fig. 2), they are straight lines, converging on the point M_m (outside the diagram):

$$T_m = T_k M^{7/6} , \tag{52}$$

$$T_0 = T_k M^{7/12} . \tag{53}$$

Stars of the main sequence have photospheres whose radii are usually smaller than R_m. To construct dependencies $T(M)$ for the photosphere, let us use formula (37). Taking into account (38), one can obtain, in the general case:

$$T_f = T_k M_\odot^i M^{k-i} . \tag{54}$$

For the equilibrium state at $k = 11/12$, we obtain three lines corresponding to three possible variants of packing of m_g-contours: into one-, two- and three-dimensional structures — i.e., at $i = 1, 1/2, 1/3$ (Fig. 2):

$$T_{f_1} = T_k\, M_\odot\, M^{-1/12}\,, \tag{55}$$

$$T_{f_2} = T_k\, M_\odot^{1/2} M^{5/12}\,, \tag{56}$$

$$T_{f_3} = T_k\, M_\odot^{1/3} M^{7/12}\,. \tag{57}$$

These lines converge on the point with coordinates close to the real parameters of the Sun, and their crossing with the outer-layer equilibrium line gives three characteristic masses: M_1, M_2 and M_3. The mass $M_1 = M_\odot^{4/5} = 13.8$ s.m., i.e., this mass also satisfies the condition $M_1 = z_0\, M_\odot$ and is equal to the mass of a red giant, which was calculated in the previous section. The mass $M_2 = 79.4$ s.m. is the largest possible mass for a main-sequence star. According to (47), this mass can give rise to an object whose mass will be 3 s.m., which corresponds to the maximal mass of a neutron star. The mass $M_3 = 277$ s.m. is the largest possible mass for a star with the most condense packing. According to our model, the structure of SO is two-dimensional; hence, stars of the main sequence are on the line T_{f_2} (bold line). Here, on the diagram *T-M*, one can also see isolines of the parameter ε, which, following (27–30), (41) and combining the constants, will look as

$$T_f = 6.86 \times 10^{-77} \frac{\varepsilon^2}{M^{2/3}}\,. \tag{58}$$

It should be noted that specific sequences of the globular-cluster stars formed from a medium with the same evolutionary parameter are also located along their own ε isolines.

When stars leave the main sequence and evolve towards lesser ε and T (to the right on the diagram), SO parameters change; particularly increasing is the envelope radius. Let us assume that beyond the line of equilibrium, $R_f = R_m$ (actually, the visible sizes of a star depend on many specific factors but we shall abstract from them in our model).

When calculating temperatures of the star envelopes (41), we implied that a part of the core radiation energy is transformed into other forms or spent in the star inner processes. But for the envelopes of giant stars, which are located to the right of the equilibrium line on the *T-M* diagram, formula (41) gives underrated results. The average density of giant stars is extremely low, and the energy of hot core radiation will insignificantly be absorbed by the rarefied atmosphere of these stars. In this case, to determine temperature of the photosphere, one can use the well-known formula for thermal radiation power, considering core as a radiation source:

$$N = \sigma T^4 S\,, \tag{59}$$

where σ is the Stefan-Boltzmann constant equal to $5.67{\times}10^{-8}$ W m^{-2}(°K)$^{-4}$. Having in mind the evident dependence of temperature on the linear size, the temperature of the photosphere can be expressed via the temperature of the core:

$$T_f = T_0 \left(\frac{R_0}{R_f}\right)^{1/2}. \tag{60}$$

Taking into account (27–30), (40) and accepting $R_f = R_m$, one can obtain, by analogy to (58),

$$T_f = 1.4 \times 10^{-55}\, \frac{\varepsilon^{3/2}}{M^{1/2}}\,. \tag{61}$$

This formula should be used when the star evolves beyond the equilibrium line and the radius of its envelope greatly increases. It is evident that the formula gives a bit overrated values of T_f. In Fig. 2, isolines plotted according to (61) are indicated as ε_{st}.

Taking into account (51) and substituting the ε_{st} expression in (61), one can obtain the line $T(M)$, along which stars turning into red giants are lined up:

$$T_{fg} = 0.192\, T_k\, M_0^{17/16}\,. \tag{62}$$

The parameters of stars with the masses M_1 and M_2 calculated for different ε values are shown in Table 2.

As for the "superstar" object, with the calculated mass $M_3 = 277$ s.m., its existence has been verified. The recently discovered star R136a1 has the following parameters: $M_0 = 265$ s.m., $R_f = 63R_\odot$ and $T_f \geqslant 40000$°K [7]. The calculated parameters of such a star — assuming it to be on the extension of the main sequence — are as follows: T_{f_2}, according to (56), is equal to 72500°K; ε from (61) is equal to 4.8×10^{38}; $R_f = R_m$ and, according to (30), is equal to $57R_\odot$. In other words, the object should be somewhere to the right of the main sequence line.

Located in the bottom part of the diagram are red dwarfs. Their typical parameters are the following: mass, $0.1, \ldots, 0.8$ s.m.; radius, $0.1 \ldots 0.85R_\odot$; temperature, below 3800°K [8, 9]. Since their radii are approximately proportional to their masses, they are on the line T_{f_1}, but their temperatures are lower, so it looks like they are on the extension of the main sequence. It is supposed that they evolve towards more condensed states, i.e., towards higher ε and T.

Lying on the lower segment of the T_{f_3} line are brown dwarfs. Their typical parameters are: mass, $0.012 \ldots 0.08$ s.m.; temperature, $3000 \ldots 300$ °K. Their radii change insignificantly over the range of masses and are approximately equal to that of Jupiter [10, 11].

At the very bottom of the diagram is the mass $M_4 = 1.95 \times 10^{-9}$ — the giant planet Jupiter. The temperature of its outer layer on the line T_{f_3} is equal, according to (57), to 123°K, i.e., it is close to the temperature of the outer atmosphere layers. The densities of Jupiter, brown dwarfs and the Sun are approximately equal; all these objects are near the line T_{f_3}.

Thus, all the types of SO are arranged logically on the *T-M* diagram.

Parameters	M_1 = 13.8 s.m		M_2 = 79.4 s.m		
	ε_1	ε_{st_1}	ε_2	ε_{st_2}	ε_{st_1}
ε	2.76×10^{38}	2.47×10^{37}	1.37×10^{39}	1.53×10^{38}	2.47×10^{37}
v_0	0.00219	0.000197	0.0061	0.00068	0.00011
R_0	0.0302	0.0302	0.0542	0.0542	0.0542
R_m	13.8	153.4	8.9	80	495
R_f	3.7	153.4	8.9	80	495
τ_0, sec	34.5	388	22.3	200	1242
τ_m, days	83	1.15×10^5	7	5037	1.2×10^6
τ_{mz}, days	6	752	0.78	63	2409
T_0, °K	2.6×10^6	2.34×10^5	7.2×10^6	8.07×10^5	1.3×10^5
T_m, °K	5710	3290	44000	21000	1370
T_f, °K	21200	3290	44000	21000	1370

Table 2: Note — radii and velocities are expressed as fractions of $R_\odot$ and c.

5.4 Variability of stellar objects

The types of variability of SO radiation are very diverse, and variability is intrinsic, to some degree, to all SO including the Sun. The most common type of variability is optical alternating variability (pulsations). According to our model, such pulsations are a natural result of the existence of oscillatory processes in the complex SO structure.

The most stable, in terms of amplitude and period of brilliancy oscillations, are pulsating stars of high luminosity — *Cepheids*, yellow giant stars [12, 13]. On the diagram *T-M*, their position would correspond to the mass M_1 on the equilibrium line T_m, where $R_f = R_m$.

Leaving the main sequence, stars become variable upon crossing the isoline ε_1 (*instability strip*), corresponding to the equilibrium parameter ε for the characteristic mass M_1. As follows from the diagram $T-\varepsilon$, the parameter ε decreases for masses larger than M_1 and increases for masses smaller than M_1 — until it reaches the isoline ε_1.

The masses of Cepheids are in the range 4 . . . 20 s.m. The minimal Cepheids mass is defined by the intersection of the isoline ε_1 and the line T_{f_2}, giving $M = 4.1$ s.m. which agrees with the value indicated in [14]. One should bear in mind that this intersection *point* on the diagram *T-M* corresponds to a *segment* on the diagram *ε-M* — from the line of equilibrium to ε_1. This segment corresponds to the initial period when the star begins to descend the main sequence. During this process, $R_f \to R_m$, which results in the star luminosity to grow. The growth is not reflected on the *T-M* diagram; on the diagram $H-R$, it corresponds to the initial segment of the star's evolutionary track.

Going on, stars evolve in the direction of lower ε values and reach the isoline ε_{st_1} (*asymptotic branch of giants, ABG*). The isoline corresponds to the equilibrium parameter ε_{st} for the standard solar mass (Fig. 1), under which the sizes of the star envelopes and the periods of their outer cycles reach their maxima. Located on ABG are *long-period variable stars* (with the period of brilliancy oscillations up to 1000 days), *semi-regular variable stars* (with the period of brilliancy oscillations up to 2000 days) and so on. Within the framework of our model, their variability can be explained not only by the existence of the outer layer period, τ_m, but also by a heterogeneity of their outer layer radiance [15, 16]. The heterogeneity results from the passage — along the star disk perimeter with the intervals of τ_{mz} — of hot (cold) zones, containing m_g-contours.

The calculated parameters R_m, T_m and τ_{mz} for M_1 (Table 2) are in a reasonable agreement with the averaged observation data for Cepheids at ε_1 and for long-period variables at ε_{st_1} [12, 17].

The parameters of SO of the mass M_2 on the line of equilibrium at ε_2 approximately correspond to those of hot supergiants PV Tel-type, with the period of pulsations from 0.1 to 1 day. On the line T_{fg} at ε_{st_2}, they correspond to the parameters of α Cyg-type super-giants, with the periods from several days to several weeks [12]. Further evolution of such stars in the direction of smaller ε values results in the formation of red super-giants.

6 Compact stellar objects

This group of SO includes white dwarfs, having the maximally compact packing of atoms, with the density ρ_0, and stellar bodies based on neutron stars, whose matter is compressed to the nuclear density ρ_j. Such objects are formed in the extreme cases, when SO evolve in the direction of either the largest ε values (when $R_f \to R_\odot$; "outer-layer state") or the smallest ones (when the envelope is shed; "core state"). In both cases, the initial oscillatory process is replaced with the rotation of the final compact object, of the mass M_p, with

the rate v_p.

At the final stage of evolution, there is, as indicated in [18], the possibility of a physical "coupling" of the star envelope with the core. Let us assume that there exists a ***process analogous to the absorption of an electron by the proton; i.e., the final compact object acquires the momentum of the outer layer, with the transition to an "excited" state***. We cannot consider the mechanism of this phenomenon within the framework of our model (moreover, the envelope and the core are considered here as different states of the same single object), so let us restrict ourselves to a formal application of the momentum conservation law:

$$M_0 v_m = M_p v_p. \tag{63}$$

6.1 White dwarfs

A white dwarf resulting from the star evolution towards lesser ε values, should inherit the parameters of the star core by the moment of the envelope shedding. For a star of the mass M_1 the parameters will be as follows: core temperature, 234000°K; period of rotation, 388 sec (Table 2). According to (47), (27) and (46), the mass, radius and mean density of white dwarfs are 0.27 s.m., 0.0082 $R_\odot$ and $2.38{\times}10^9$ kg/m^3 respectively. Indeed, very young white dwarfs can be observed in the X-ray range; the periods of their pulsations are in the range of tens to thousands of seconds, and they have typical sizes and densities being in agreement with the calculated parameters [12, 19, 20].

A white dwarf resulting from the evolution of a low-mass star towards larger ε values (without shedding of the envelope) should have the mass $M_p \approx M_0$. Then, its $v_p \approx v_m$.

Having in mind (29), (31) and (36), let us represent v_m as

$$v_m = cM_0^{2k-2/3} \tag{64}$$

and the period of rotation as

$$\tau_m = \frac{R_0}{v_m} = 2.51 M_0^{1-2k}. \tag{65}$$

At $z = 1$ and $k = 2/3$, an object of the mass 0.27 s.m. will have the following parameters: $v_m/c = 6.7 \times 10^{-5}$; $\tau_m = 308$ sec; and the energy of radiation, according to (42), equal to 0.034 keV ($T = 79000$°K). Here, the calculated parameters are, too, typical for a young white dwarf. As the object on the *T-M* diagram shifts to the right, the parameter k grows, which corresponds to the decline of the rotary velocity and temperature of the white dwarf.

On the diagram "*spectrum-luminosity*", the zone of white dwarfs seems much narrower than that on the diagram *T-M*, since their luminosity is determined by the radius, which, according to (27), is proportional to cubic root of the object mass.

6.2 Neutronization

In the context of our model, the process of neutronization can be represented as a loss of stability of the structure of m_g-contours and the transition of the structure (through its inversion along the vertical axis) from the plain two-dimensional into a one-dimensional configuration, which is energetically more favorable. Let us assume that the result will be a single m_g-contour or just a single vortical tube (neutron object).

Roughly, the parameters of such a primitive object can be defined as in Chapter 3. Placing the parameter R along the vertical axis and considering $z = 1$, one can obtain:

$$v_n = \frac{fM_n c}{\varepsilon}, \tag{66}$$

$$d_n = \frac{\varepsilon^2 R_\odot}{f^2 M_n}, \tag{67}$$

$$R_n = \frac{fM_n R_\odot}{\varepsilon}, \tag{68}$$

$$\tau_n = 2.51 \frac{(\varepsilon/f)^3}{M_n^2}. \tag{69}$$

Rotary velocity cannot exceed the speed of light. Therefore, at $v_n \leqslant c$, $\varepsilon \geqslant fM_n$. Thus, for compact objects, the parameter k in (36) should be $\leqslant 1$ (in any event, as follows from the comparison of the calculated and actual data, k cannot be much larger than 1). Let us limit ourselves to defining parameters at $v_n = c$. Expressing ε from (66), one can obtain:

$$d_n = M_n R_\odot, \tag{70}$$

$$R_n = R_\odot, \tag{71}$$

$$\tau_n = 2.51 M_n. \tag{72}$$

It should be noted that a high-frequency modulation with τ_n up to 10^{-6} sec is present on the radiation diagrams of some neutron stars — pulsars [6].

As the evolutionary parameter grows, the sizes of a neutron object shrink along the axes, and on the line of degeneration, at $z = 1$, one can rewrite expressions (67–69), having in mind (35), in the following form:

$$d_n = R_n = M_n^{1/3} R_\odot, \tag{73}$$

$$\tau_n = \frac{R_\odot}{c} = 2.51 \text{ sec}. \tag{74}$$

Of course, this scheme is ideal. In reality, the objects based on neutron stars are in some intermediate state, and in the general case,

$$d_n = M_n^j R_\odot, \tag{75}$$

where $j = 1/3, \ldots, 1$ is a coefficient taking account of the object packing (shape).

It seems that the neutron state should be realized, to some extent, in the core of any star — and this can be proved. Let

represent the mass of a single vortex tube as that of a cylinder of the length R_n and radius d_n. Taking into account (70) and (71),

$$M_n\, M_m = \rho_n\, (M_n R_\odot)^2\, R_\odot, \tag{76}$$

where ρ_n is the vortex tube averaged density. Let us assume that ρ_n cannot exceed the nuclear density ρ_j, which shall be considered equal to $m_p/r_e^3 = 7.47 \times 10^{16}$ kg/m^3, where m_p is the mass of a proton. Then, as follows from (76),

$$M_{min} \geqslant \frac{M_m}{\rho_j R_\odot^3}\,, \tag{77}$$

which, upon substitution of values, gives $3.19{\times}10^{-8} M_m$. This mass corresponds to 0.016 solar masses or 17 Jupiter masses — exactly what the smallest cosmological mass, which is still considered a star, should be.

6.3 Masses of "black holes"

The diagrams ε-M and T-M show the boundary of a critical mode, where the rotary velocity of a vortex tube reaches that of light. On the diagram ε-M, the ray indicating the critical situation looks — taking into account that M_n is the mass of the compact object to be raised — as

$$\varepsilon = f M_n = f M^{11/8}\,. \tag{78}$$

On the diagram T-M, the same ray has — upon substitution of ε in (61) — the following form:

$$T_{f\,lim} = T_k\, M^{25/16}. \tag{79}$$

As follows from this construction, a ray segment is limited by the ordinates of the masses M_2 and M_3 and intersection with the isolines ε_{st_1} and ε_{st_2} — there are almost perfect ternary points of intersection. It is these masses that give rise to neutron objects with the masses, according to (47), $3, \ldots, 16$ s.m., which are the sources of hard X-ray radiation and *candidates for the star mass "black holes"* [18].

Indeed, for giant stars of a mass $M_2{-}M_3$, the critical mode begins before the moment they reach the asymptotic branch of giants (super-giants). With further decrease of the parameter ε, a star should release the excess of angular momentum — probably, by means of dropping the excess mass, which can be interpreted as shedding of the envelope with the formation of *supernova*. Next, the star core of a mass $M_n < \varepsilon/f$ transforms to an object which presently is classified as the "black hole" candidate. If neutronization of SO occurs far beyond the critical boundary (at low ε values), the mass of the emerging object will be very small. The latter might be one of the causes of the supernova remnants to contain few compact objects.

6.4 Radio pulsars

In our model, the simplest radio pulsar is a vortex tube which, by definition, is in the region Y ("boson"). The vortex tube is a macro-oscillator or radiator, with oscillations forming as longitudinal vibrations along the entire tube, while propagating to the X region as a cross wave from their source (the entrance of the vortex tube to the Y region; orifice) [2]. Presumably, radiation in the observable region X has a wavelength λ_p commensurable with the characteristic size of a single element of the vortex tube. A vortex tube, according to (22), consists of $n = \varepsilon$ single vortex threads — therefore, the characteristic linear size of a single element (region of radiation) will amount, under the condition of maximally compact packing of vortex threads in three dimensions, to

$$d_p = \varepsilon^{1/3} r_e\,. \tag{80}$$

The speed of vortex tube rotation can be expressed as a proportion of light speed — using the analogies described in Chapter 3:

$$\mathrm{v}_p = c\,\frac{\lambda_k}{d_p}\,. \tag{81}$$

Taking into account (36) and combining the constants, one can find the period of a pulsar:

$$\tau_p = \frac{d_p}{\mathrm{v}_p} = \frac{\varepsilon^{2/3} r_e^2}{c\lambda_k} = 282.5\, M_p^{2k/3}\ \mathrm{sec}\,. \tag{82}$$

Along the vortex tube of the pulsar, radiation is formed by m_i-zones, the number of which is determined by the pulsar mass. The averaged profile of the radiation pulse is a result of random superposition of many single pulses. Therefore the duration of the generalized pulsar pulse τ_{p_i} can be in the range from the duration of a single m_i-zone pulse to the total duration of pulses of all the zones, i.e. from r_i/v_{0i} to $z_i\, r_i/\mathrm{v}_{0i}$. Having in mind (18), (19) and (21),

$$\tau_{pi} = 2.51 M_p^{1/2\ldots1/4}\,. \tag{83}$$

For a pulsar, the standard mass is taken as 1.4 of that of the Sun. Then the pulsar period at $k = 2/3 \ldots 1$ will be, according to (82), in the range from 0.97 to 0.045 sec; and the duration of the generalized pulse will be, according to (83), in the range from 0.1 to 0.0042 sec, this corresponding to the temporal parameters of the majority of radio pulsars [21–23].

Radio radiation of pulsars covers a broad range and is extremely heterogeneous in time, intensity and frequency. Nevertheless, there are stable averaged spectra of energy distribution over frequency obtained by multiple instant measurements of radiation at different frequencies over large periods of time.

Let $\lambda_p = 2\pi d_p$, then the *frequency of radiation*, taking into account (80–82), will be as follows:

$$\nu_p = \frac{c}{2\pi d_p} = \frac{c}{2\pi\varepsilon^{1/3} r_e}\ \mathrm{Hz}, \tag{84}$$

which, having in mind (82), can be reduced to

$$\nu_p = 1.77\tau_p^{-1/2} \text{ GHz}. \tag{85}$$

Since d_p is the minimal parameter provided that m_i-zone are packed most compactly, expression (84) will give *maximal* frequencies. However, the averaged spectrum extends far in the region of low frequencies and has an energy maximum. On the basis of our model, this fact can be accounted for by pulsation of the vortex tube in the limits of d_n, formula (75), and the existence of its optimal packing, less than 3, which the pulsar assumes most of the time. As indicated in [3], it may be the fractal dimension $e = 2.72$. In this case, the power of the parameter ε will be equal to $1/e$, and, as follows from (84), $\nu_p/\nu_m = \varepsilon^{0.0345}$. Having in mind (82), one can obtain, for the frequency of the maximum:

$$\nu_m = 0.0804\tau_p^{-0.55} \text{ GHz}. \tag{86}$$

Formulas (85) and (86) are virtually identical to the interpolation formulas given in [23].

Although radiation of pulsars is not thermal, the *power of radiation* N_p can be determined on the basis of a formal use of the Boltzmann formula for thermal radiation of black body under the following conditions:

- taken as the area of the radiating surface is the cross-section of the vortex tube, $S = d_p^2$;
- taken as the effective temperature T_{ef} is the temperature corresponding to the radio frequency T_ν increased proportionally to the relative length of the vortex tube (i.e. proportionally to the ratio of the initial-object* radius to the diameter of the vortex tube, $T_{ef} = T_\nu R_0/d_p$).

Since, having in mind (39, 40), $T_\nu = T_k\lambda_k/d_p$, one can obtain, taking into account (36) and (80) and combining the constants,

$$T_{ef} = 1.06\times 10^7 M_p^{1/3-2k/3}. \tag{87}$$

Finally, after calculating the constants, we get an expression for N_p:

$$N_p = \sigma T_{ef}^4 S = 1.45\times 10^{20} M_p^{4/3-2k} \text{ W}. \tag{88}$$

Thus, our model predicts that at $k \to 2/3$, a radio pulsar should have a *lower* limit for radiation power (N_{min}), which the pulsar will be approaching as its rotation is getting slower. The limit N_{min} is equal to 1.45×10^{20} W and does not depend on the pulsar mass. At $k = 1$, expression (88) will give an upper limit N_p, which is dependent on the pulsar mass. The limits do exist [23], and no pulsars has been found at the luminosity below N_{min}.

On the basis of (82) and (88), a dependence $N(\tau_p)$ can be constructed (Fig. 3), which corresponds to the correlation given in [23]. To cover the zone of millisecond pulsars, the dependence is plotted in the range of masses $3\ldots 0.016$ s.m. — i.e. up to the minimal masses still able to neutronize (see Chapter 6.2). (The question on the range of radio pulsar masses is still open, since they can be determined only in rare cases).

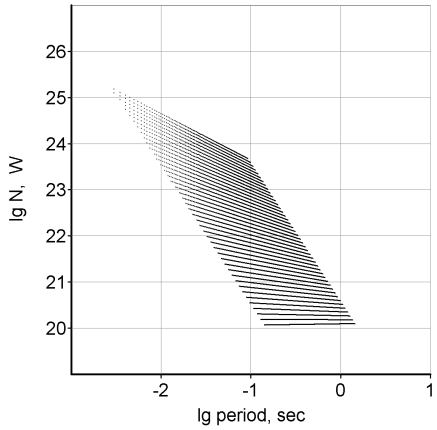

Fig. 3: Dependence of the radio pulsar radiation power on its period. $M_p = 3\ldots 0.016$ s.m., $k = 0.66\ldots 1$.

6.5 Excited states. Gamma-pulsar

Essentially, pulsar or vortex tube is a lengthy solenoid. In our model, the full length of a thread $z_i\, l_i$ does not depend, according to (18) and (20), from the mass and is equal to $R_\odot$; the length of a turn is, in general case, $\pi M_p^j R_\odot$, and the number of turns in the initial state is $\mathrm{N} = M^{-j}/\pi$.

Let us assume that the configuration of the vortex tube can change — e.g., upon the formation of a secondary spiral structure. In this case, the initial radius can diminish to the minimal radius of the vortex tube d_p, and the number of turns can grow to the number $\mathrm{N}_m = R_\odot/\pi d_p$. Then, taking into account (36) and (80),

$$\frac{\mathrm{N}_m}{\mathrm{N}} = 1.66\times 10^9 M_p^{j-k/3} = 10^5\ldots 10^9, \tag{89}$$

which will result in the correspondingly increased magnetic power and activity of the pulsar.

This state can be considered as an "excited" state of the radio pulsar. If the effective temperature grows proportionally as well, the energy corresponding to this increase will be transferred into the gamma range. Multiplying (87) by (89) and taking into account that for the vortex tube $j = 1$, one can obtain

$$T_{ef} = 1.76\times 10^{16} M_p^{4/3-k}. \tag{90}$$

Thus, at certain combinations of the parameters, formula (90) will give (upon conversion into electron-volts) values up to $10^{13}\ldots 10^{14}$ eV. This explains, for example, the observed gamma radiation of the famous pulsar in the Crab Nebula (more than 10^{12} eV). Ratio (89) serves estimation purposes, yet it can be used in other cases as well.

*The object of the initial mass (before neutronization).

6.6 X-ray pulsars

Massive stars give rise to neutron objects. Let us assume that such an object can be formed at any stage of star evolution, with the envelope momentum transferred to this newly formed object. Let us also assume that further evolution of this system as a whole can go both to the right (up to the state of outer layer) and left (up to the state of core) of the equilibrium line with the eventual formation of an *x*-ray pulsar of the mass M_p.

As a rule, X-ray pulsars do not radiate in the radio range. According to the model considered, we can assume this residual compact object to be already in the neutron state, while its vortex tube (or a part of the tube) excited at the expense of an additionally absorbed momentum to be still in the X region and to radiate in the X-ray range.

Let us determine the pulsar's parameters. Having in mind (63) and (64) and substituting, according to (47), $M_p^{8/11}$ for M_0, one can obtain for the pulsar:

$$\mathrm{v}_p = cM_p^{1.454k-0.7575}, \tag{91}$$

$$E_p = 511 M_p^{1.454k-0.7575}\ \mathrm{keV}. \tag{92}$$

The pulsar period d_n/v_p, in the case of arbitrary pulsar form, will be equal to

$$\tau_p = \frac{M_p^j R_\odot}{\mathrm{v}_p} = 2.51\, M_p^{0.7575-1.454k+j}. \tag{93}$$

It should be noted that at $k = 0.75$ and $j = 1/3$, the M_p factor in (93) will be zero and $\tau_p = 2.51$ sec — the same period for any mass.

Let us consider the pulsar radiation to be mainly thermal. Then, one can calculate its power according to the Boltzmann formula, taking as the *radiating surface* that of the vortex tube of the length R_0 (i.e. $S = \pi d_p R_0$). In this case — analogously to (88), taking into account (27), having in mind $T_p = (T_k E_p)/511$ and after transformations — one can obtain, for an X-ray pulsar:

$$N_p = 1.22 \times 10^{38} M_p^{6.15k-2.7}\ \mathrm{W}. \tag{94}$$

The parameters of most of the known X-ray pulsars fit into the intervals calculated according to (92–94) for the standard mass 1.4 s.m. at $k = 2/3 \ldots 1$ and $j = 1/3 \ldots 1$: $\tau_p = 0.002 \ldots 260$ sec, $E_p = 0.07 \ldots 35$ keV, $N_p = 10^{20} \ldots 10^{30}$ W. Periods of more than 1000 sec are characteristic for small masses or for the cases when momentum is not fully transferred from the outer layer to the emerging compact object. Thus, there exist restrictions on the magnitudes of periods, energy and radiation power; and it is them that explain, to a certain degree, the partially non-thermal form of the pulsars energy spectrum (a cut-off in its high-energy region) [18, 24].

Radiating in the X-ray region are also some radio pulsars. Let us demonstrate the adequacy of our model on these objects — on the example of correlation between *x*-ray luminosity and the parameter $(d\tau/dt)/\tau^{3.5}$, given in [23]. The period derivative $d\tau/dt$, the rate of deceleration of pulsar rotation, is determined from observations. In our model, rotation slowdown is determined by the general process of evolution of the object's medium, i.e., by the parameter k. So let us use a derivative of the period in respect to k, considering the parameter j constant and replace the aforementioned expression by corresponding equivalent. In the end, differentiating (93) and combining the constants, one can obtain

$$\frac{d\tau_p/dk}{\tau_p^{3.5}} = -3.35 \lg M_p\, \tau_p^{-2.5}. \tag{95}$$

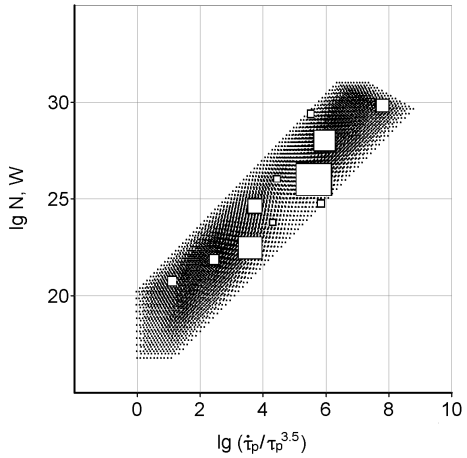

Fig. 4: Dependence of the radio pulsar *x*-ray luminosity on the parameter $(d\tau_p/dk)/\tau_p^{3.5}$. $M_p = 3 \ldots 0.3$ s.m., $k = 0.66 \ldots 1$, $j = 0.68 \ldots 0.73$. Observation data are taken from [23].

Fig. 4 shows the dependence of X-ray luminosity of a radio pulsar on the parameter $(d\tau_p/dk)/\tau_p^{3.5}$ in the range of masses $3 \ldots 0.3$ s.m. The dependence fits the observation data at the values of the parameter $j = 0.68 \ldots 0.73$. In Fig. 4, the size of squares is approximately proportional to the number of observation points (41 points in total according to [23]). In our case, the derivative does not require a scale coefficient to satisfy the initial conditions.

It is known that during *outbursts*, the power of radiation (luminosity) reaches a magnitude of the order of 10^{32} W and higher [25]. According to our model, such an increase in luminosity can be explained by periodical excitation of the vortex tube (see Section 6.5). In this case, multiplying (94) by (89), one can obtain

$$N_{pm} = 2.03 \times 10^{47} M_p^{5.82k+j-2.7}. \tag{96}$$

Formula (96) gives rational results. For the mass $M = 1.4$ s.m., N_p will reach, depending on the parameters, magnitudes of $10^{38} \ldots 10^{39}$ W, which agrees with the power of the giant gamma-ray outburst from the source SGR 1900-14, which was registered in August 1998 (about 10^{38} W) [27].

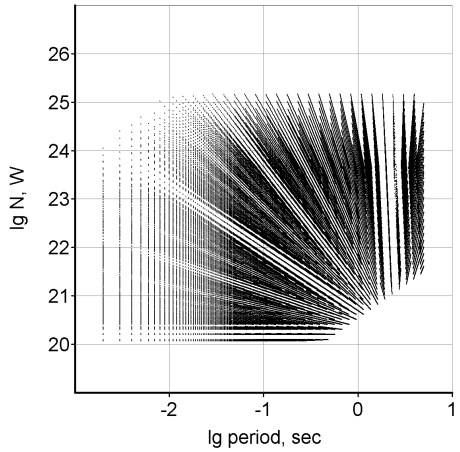

Fig. 5: The solution region: dependence of the radio pulsar radiation power on its period. $M_p = 3 \ldots 0.016$ s.m., $k = 0.66 \ldots 1$, $j = 0.33 \ldots 1$.

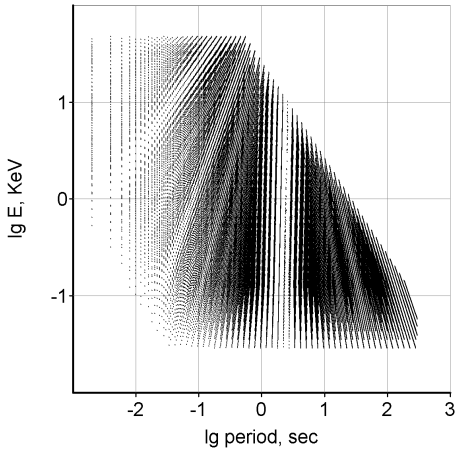

Fig. 6: The solution region: dependence of the X-ray pulsar radiation energy on its period. $M_p = 3 \ldots 0.3$ s.m., $k = 0.66 \ldots 1$, $j = 0.33 \ldots 1$.

It would be interesting to get independent estimates of the mass of compact objects, which, as one can see, have a similar origin. Let us assume that in the process of their possible inter-transformations, their masses and periods change insignificantly. Let the X-ray and radio pulsar periods are equal in the marginal cases — when the initial SO, giving rise to a compact object, evolves towards the largest or smallest ε values.

Let us consider the case when evolution goes towards larger ε. With ε increasing, the mass M_p should grow and at $z \to 1$ become equal to the original mass M_0 (Fig. 1). Perhaps, such a process should be associated with *accretion in binary star systems*. Proceeding to the mass M_0, let us substitute $M_0^{11/8}$ for M_p in (91). Then $d_n = M_0^j R_\odot$ and (93) will take a form of

$$\tau_p = 2.51 M_0^{1.042-2k+j}. \tag{97}$$

Equating (82) to (97) for the periods, combining the constants and making transformations, one can obtain in the end:

$$\lg M_0 = \frac{2.052}{1.042 - 2.667k + j}. \tag{98}$$

In the limit, $k = 2/3$ and $j = 1/3$ (sphere), then $M_0 = 8 \times 10^{-6}$ or 4 s.m. This mass can be considered as the total one of a *low-mass binary star system* containing an X-ray pulsar, this being in agreement with the accepted estimate (2.5 s.m. + 1.4 s.m.) [18]. Such a pulsar will have a relatively hard X-ray radiation [25], and, with the growth of the parameters j, its period will decrease.

The obtained mass value is, in fact, coincides with the minimal mass of a Cepheids (see Section 5.4). Thus, an SO with the mass 4 s.m. can evolve both to the right of the equilibrium line (shedding the envelope) and to the left (forming a binary star system). In both cases, a compact object will be formed at the end of evolution, and one can suppose that the stellar mass of 4 s.m. is the *minimal mass* able to give rise to neutron stars.

Let an X-ray pulsar evolve towards lesser ε values. Equating expressions (82) and (93), one can obtain

$$\lg M_p = \frac{2.052}{0.7575 - 2.121k + j}. \tag{99}$$

In the limit, $k = 1$ and $j = 1$ (vortex tube), then $M_p = 2.3 \times 10^{-6}$ or 1.15 s.m. Here, we have got a typical pulsar mass. Such a pulsar will have a relatively soft X-ray radiation, and with the parameter j growing, the pulsar period will increase. Such objects can correspond to *single neutron stars* [26]. Indeed, as follows from the observation data, pulsars of binary systems will mainly speed up their rotation, whereas single objects will slow down.

The properties of SO are determined by the totality of their parameters; that is why two-parameter diagrams always have a wide scatter of experimental points. Let us represent the solution region of the dependence $N(\tau_p)$ for radio pulsars more extensively — expressing its period according to (93), which contains the parameter j, and considering some radio pulsars evolved from the X-ray ones, with their periods being approximately the same (Fig. 5). The region of observation values [23] fits well the solution region.

Analogously, using formulas (92) and (93), one can plot a solution region of the dependence $E(\tau_p)$ for the X-ray pulsars (Fig. 6). Clusters on the images may indicate regions where pulsars have preferable parameters — e.g., the right bottom part in Fig. 6 may indicate, by the combination of parameters, a region of single neutron stars.

There appears a question: can slow X-ray pulsars transform into radio pulsars, whose period will not exceed several seconds? One can suppose that comparatively to radio pulsars, X-ray ones have an excessive angular momentum (since their radius in the region X is much larger than that of ra-

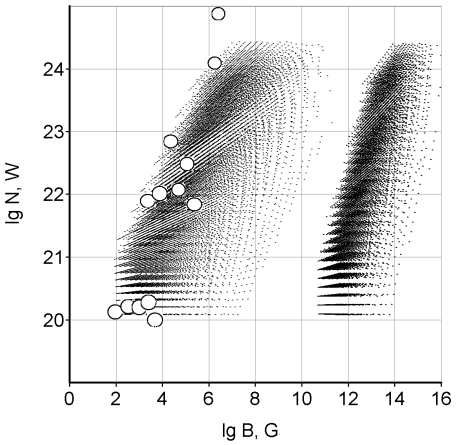

Fig. 7: The solution region: dependence of the radio pulsar radiation power on its magnetic field — $N(B)$ to the left; $N(B_m)$ to the right. $M_p = 2 \ldots 0.2$ s.m., $\tau_p = 0.003 \ldots 3$ sec, $k = 0.66 \ldots 1$, $j = 0.33 \ldots 1$. Observation data are taken from [23].

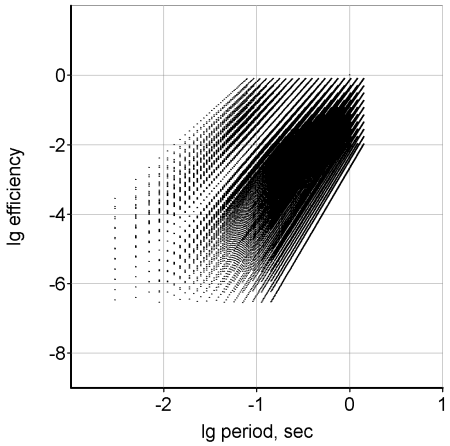

Fig. 8: The solution region: dependence of the efficiency of transformation of rotation energy in-to radio radiation on the pulsar period (initial state). $M_p = 3 \ldots 0.016$ s.m., $k = 0.66 \ldots 1$, $j = 0.33 \ldots 0.55$.

dio pulsars in the region Y, and as they "submerge" into the region Y, their period shortens).

Thus, ***it can be supposed that gamma, X-ray and radio pulsars are different forms of excited vortex tube or, using another analogy with the microcosm, three species of neutrino. The primary state — radio pulsar — possesses only the initial angular momentum of the vortex tube or spin***.

6.7 Magnetic properties of pulsars

Our model explains the correlation between the magnitude of the magnetic field B and other pulsar parameters. According to SI definition, for a lengthy solenoid, $B = \mu\mu_0\, nI$, where n is the number of turns per unit of length, I is the current strength and μ is the relative magnetic permeability.

The initial solenoid length is equal to R_0. Let $n = \mathrm{N}/R_0$. Let us define the coefficient μ as the compactness of the solenoid coil in the initial state $\mathrm{N}d_p/R_0$. The current strength I in the "Coulombless" form is $z_e m_e\, c(R_\odot/r_e) \times 1/[\mathrm{sec}]$ (see Section 2), where z_e is the number of single charges per coulomb, equal to $1/e_0$.

In our model, SI units for B are m^{-1}. To switch from SI to the Gaussian system of units, introduction of an additional factor of 10^{-4} is needed. Opening the expressions for μ_0, ε_0 and $R_\odot$, taking into account that $\mathrm{N} = M^{-j}/\pi$, as well as (27), (36) and (80), and making transformations, one can finally obtain

$$B = 1.27 \times 10^{-4} M_p^{k/3-2j-2/3}\ \mathrm{G}. \qquad (100)$$

Many radio pulsars have larger B values. For the excited state, multiplying (100) by (89), we will have

$$B_m = 2.1 \times 10^{5} M_p^{-j-2/3}\ \mathrm{G}. \qquad (101)$$

Fig. 7 shows the solution regions for the dependences $N(B)$ (to the left) and $N(B_m)$ (to the right) calculated according to formulas (88), (100) and (101) in the range of masses $2 \ldots 0.2$ s.m. and periods $0.003 \ldots 3$ sec. The figure also represents the observation data for the pulsars with small B values taken from [23]. Masses and periods are connected using formula (93), which contains the parameter j. It is known that according to the strength of their magnetic field, pulsars are clustered near values of the order of 10^9 and 10^{13} G [18], which agrees, in general, with the distributions obtained.

To analyze pulsar parameters, the function $\eta(\tau_p)$ is also used, which includes the magnetic force B [23]:

$$\eta = \frac{3N_p\, c^3 \tau_p^4}{8\pi^4 B^2 R_*^6}, \qquad (102)$$

where η is the pulsar efficiency, i.e., the effectiveness of transformation of the pulsar rotation energy into radio radiation.

According to [23], formula (102) takes $R_* = 10^6$ cm. For more objectiveness, let us replace this constant with the diameter of the vortex tube according to (75). Having in mind (82), (88) and (100), let us transform (102) to the form (in the Gaussian system):

$$\lg \eta = 8.5 + (2.667 - 2j) \lg M_p\,. \qquad (103)$$

Together with formula (82), this gives the region of $\eta(\tau)$ solutions for radio pulsars (Fig. 8). Since $\eta < 1$, there are limitations for some combinations of the parameters. In the accepted, according to [23], range of η values, the parameter j is limited by the range $0.33 \ldots 0.55$, which is characteristic for pulsars with small B values. The orientation of clusters on the diagram indicates the increase of η with the growth of the period.

Analogously, substituting the parameter B_m into (102), one can obtain

$$\lg \eta = -11.9 + (0.667k - 4j + 2.667) \lg M_p. \qquad (104)$$

In this case (Fig. 9), in the accepted range of η values, the parameter j is limited by a narrow range of large values,

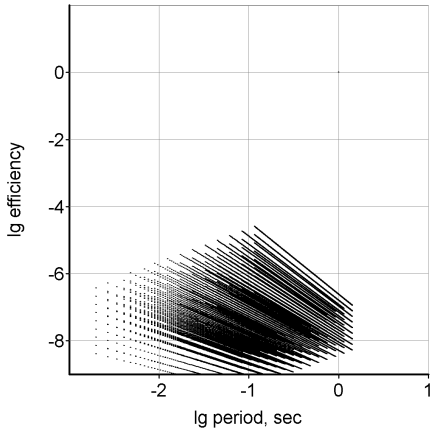

Fig. 9: The solution region: dependence of the efficiency of transformation of rotation energy in-to radio radiation on the pulsar period (excited state). $M_p = 3 \ldots 0.016$ s.m., $k = 0.66 \ldots 1$, $j = 0.94 \ldots 1$.

$0.94 \ldots 1$, which corresponds to pulsars with a strong magnetic field. In this range of parameters, η will grow as the period decreases. These solution ranges complement each other and agree with the body of the observation data of the diagram $\eta(\tau)$ given in [23]. Thus, there are at least two pulsar populations, with different magnitudes of their magnetic field and different form factors (parameter j), which was also indicated in [23].

From (101), one can find that the magnitude of the pulsar magnetic field can reach $10^{14} \ldots 10^{15}$ G. Such a growth of the magnetic field also explains the phenomenon of *magnetars* [27, 28].

As follows from our model — and it is getting evidence now — there are no essential differences between magnetars and X-ray pulsars. For example, the sources SWIFT J1822.31606 [29] and PSR J18460258 [30] possess features of both objects.

7 Conclusion

Thus, our model, which is built exclusively on the balances of basic interactions, describes different kinds of stellar objects. It is shown that SO features are mainly determined by their masses and the state of the evolving medium that they are made of. Together with the basic constants, these parameters (M and ε) determine the evolutionary behavior of stellar objects and the very existence of the well-known Hertzsprung-Russell diagram. In a number of cases, they are sufficient for the calculation of basic SO parameters: the mass of the final compact objects, radiation energy, radiation power and periods or rotation.

The model reveals analogies between the macro- and microlevels of matter: cosmological masses and elementary particles.

Indeed, the ***general range of stellar masses can be roughly divided into three subranges — by the analogy with the three families of elementary particles***:

- stars with masses less than 4 s.m., which in the end of evolution will become white dwarfs;
- giant stars with masses $4 \ldots 79$ s.m., which in the end of evolution will give raise to neutron stars;
- super-giant stars with masses $79 \ldots 277$ s.m., which in the end of evolution will give raise to X-ray sources — candidates for black holes.

It is the ***stars of small masses and their final states (cold white dwarfs, "protons") that are the "first family" of stellar population***. They make the majority of it and are stable on the cosmological scale, since their lifetimes are immeasurably longer than the lifetimes of other stellar objects.

Hopefully, the results obtained and the presented model can be useful for further theoretical studies in the field.

Submitted on: June 26, 2012 / Accepted on: October 10, 2012

References

1. Belyakov A.V. Charge of the electron, and the constants of radiation according to J. A. Wheeler's geometrodynamic model. *Progress in Physics*, 2010, v.4, 90–94.
2. Belyakov A.V. Macro-analogies and gravitation in the micro-world: further elaboration of Wheeler's model of geometrodynamics. *Progress in Physics*, 2012, v.2, 47–57.
3. Belyakov A.V. On the independent determination of the ultimate density of physical vacuum. *Progress in Physics*, 2011, v.2, 27–29.
4. Novikov I.D., Kardashev N.S., Shatskiy A.A. Multicomponent Universe and astrophysic of the "wormhole". *Uspekhi-Physics*, 2007, v.177(9), 1017–1023.
5. Beck P.G., Montalban J. et al. Fast core rotation in red-giant stars as revealed by gravity-dominated mixed modes. *Nature*, January 2012, v.481, 55–57.
6. Narlikar J. Violent Phenomena in the Universe. Oxford University Press, Oxford, 1984.
7. Crowther P.A. The R136 star cluster hosts several stars whose individual masses greatly exceed the accepted 150 $M_\odot$ stellar mass limit. *Monthly Notices of the Royal Astronomical Society*, 2010, v.408(2), 731–751.
8. Burrows A., Hubbard W.B., Saumon D., Lunine, J.I. An expanded set of brown dwarf and very low mass star models. *The Astrophysical Journal*, 1993, v.406, no.1, 158–171.
9. Kaltenegger L., Wesley A. Transits of earth-like planets. *The Astrophysical Journal*, 10 June 2009, v.698, 519–527.
10. Spiegel D.S., Burrows A., Milsom J.A. The Deuterium-burning mass limit for brown dwarfs and giant planets. ariv: astro-ph/1008.5150.
11. Michael C.L. et al. CFBDSIR J1458+1013B: a very cold (>T10) brown dwarf in a binary system. ariv: astro-ph/1103.0014.
12. Kholopov P.N., Samus N.N., Goranskiy V.P. et al. Main catalog of the variable stars. v. I-III. Nauka, Moscow, 1985–1987 (in Russian).
13. Berdnikov L.N., Samus N.N. Studies of classical cepheids. *Astronomical & Astrophysical Transactions*, 1999, v.18(2), 373–384.
14. Berdnikov L.N., Dambis A.K. Cepheids and RR Lyr variables. Present star astronomy. Sternberg Astron. Inst., Moscow, 16 June 2011 (in Russian).
15. Mennessier M.O., Mowlavi N., Alvarez R., Luri X. Long period variable stars: galactic populations and infrared luminosity calibrations. *Astronomy & Astrophysics*, 2001, v.374, 968–979.

16. Hampton M., Gregory W.H. et al. HD 12545, a study in spottedness. *Publication of the Astronomical Society of the Pacific*, January 1996, v.108, 68–72.

17. Le Bertre T., Lebre A., Waelkens C. (Eds.). Asymptotic Giant Branch Stars. *Proc. 191st Symp. IAU*, 1999.

18. Svertilov S.I. Cosmic X-ray and gamma-ray radiation. Skobeltzin Inst. Nucl. Research, Moscow, April 2006 (in Russian).

19. Shapiro S.L., Teukolcky S.A. Black holes, white dwarfs and neutron stars. v.1–2. Nauka, Moscow, 1985.

20. Kepler S.O., Vauclair G., Nather R.E., Winget D.E., Robinson E.L. G117-B15A — how is it evolving? *White dwarfs; Proceedings of IAU Colloquium 114th*, August 1988, (A90-32719 13-90).

21. Manchester R., Talor D. Pulsars. Nauka, Moscow, 1980.

22. Matveenko L.I., Usov V.V. Physics of the Cosmos. Nauka, Moscow, 1986 (in Russian).

23. Malov I.F. Radio pulsars. Nauka, Moscow, 2004 (in Russian).

24. Tsygankov S.S., Lutovinov A.A. Studies of x-ray pulsars with space observatories. *Proceedings of the VIII-th Young Scientist Conference*, 2005, 226–228 (in Russian).

25. Aleksandrovich N.A., Borozdin K.N., Arefjev V.A., Sunyaev R.A., Skinner D.K. Observations of the X-ray transit pulsar-burster GRO J1744-28 with the telescope TTM of the orbital observatory "MIR-KVANT". *Soviet Astron. Journal Letters*, 1998, v.24, no.1.

26. Popov S.B., Prohorov M.E. Astrophysics of the isolated neutron stars: radio-quiet neutron stars and magnetars. Sternberg Astron. Inst., Moscow, 2002 (in Russian).

27. Kouveliotou C., Duncan R.C., Thompson C. Magnetars. *Scientific American Russian Edition*, 2003, no.6 (in Russian).

28. Tsygankov S.S., Lutovinov A.A. Universe magnetic heart. *Priroda*, 2011, no.1, 10–18 (in Russian).

29. Scholz P., Ng C.-Y., Livingstone M.A., Kaspi V.M., Cumming A., Archibald R. SWIFT J1822.31606: post-outburst evolution of a nearby magnetar. arXiv: astro-ph/1204.1034.

30. Gavriil F.P., Gonzalez M.E., Gotthelf E.V., Kaspi V.M., Livingstone M.A., Woods P.M. Magnetar-like emission from the young pulsar in Kes 75. *Science*, 28 March 2008, v.319, no.5871, 1802–1805.